EXPERIMENTAL STUDY OF SATURATED POOL BOILING HEAT TRANSFER OF I_E WATER

CHUNSING WANG

Originally published as *Physical, Chemical and Biological Properties of Stable Water Clusters*,
Proceedings of the First International Symposium.
Reprinted here by permission of
World Scientific Publishing Company, 1998.

Pool boiling, of saturated I_E water clusters, at one atmosphere was investigated. In the experiments, a vertical copper surface with a mirror surface was used. The wall heat flux and superheat were determined with the help of thermocouples embedded in the test block. The still photographs were taken during the experiments. The nucleate boiling, critical and film boiling heat fluxes as function of wall superheat patterns for I_E water are compared with these for water. It is concluded that I_E water changes bubble formation, flow pattern above heating surface, and enhances boiling heat transfer as compared to plain water.

1. INTRODUCTION

Boiling is a phase heat transfer process that involves more than a knowledge of the usual heat transfer modes: conduction, convection and radiation. It continues to attract attention because it allows engineers to remove a tremendous amount of heat from small spaces. Rocket engines, superconductors, jet aircraft engines, electronic devices and nuclear reactors all produce a large amount of heat that has to be removed efficiently by means of a new boiling technology. A precise evaluation of the boiling process is very important for component cooling, in these high density energy systems.

The wall superheat is the temperature difference between the heater surface and the ambient liquid. As the surface temperature is increased, until a certain thermal condition is met, the incipient nucleation occurs. The vapor bubbles begin to form on the cavities of the boiling surface. This is called the discrete bubble regime or partial nucleate boiling regime. In this regime, the frequency and number density of the bubbles increase when surface superheat is increased, thereby resulting in a higher heat flux. As wall heat flux or superheat increases further, the frequency of bubble release and the number density of active cavities also increase. At a certain bubble release frequency, the distance between rising bubbles is equal to, or less than, one bubble diameter and the vapor bubbles merge to form columns.

As the superheat increases further, the number of vapor columns on the surface increases. The bubbles on top of the vapor columns begin to merge with bubbles of neighboring vapor columns to form bigger vapor structures called vapor mushrooms. Vapor appears to jet away from the heating surface. Thus massive vapor mushrooms[1] and columns can be seen near the heating surface. This is called fully developed nucleate boiling. Then, the maximum heat flux occurs at a peak and is called the critical heat flux or maximum heat flux. The critical heat flux occurs either because of the limit on vapor removal rate or vapor generation rate on the surface.

After the critical heat flux, the surface heat flux is decreased with increasing surface superheat. This is called transition boiling regime. Transition boiling is believed to be a mixed model of nucleate and film boiling. Liquid-solid as well as vapor-solid contacts must therefore exist and have indeed been observed in experiments. Surface heat flux reaches a minimum as surface temperature is further increased. This is called minimum film boiling condition.

When surface temperature becomes higher than a minimum boiling condition temperature, the surface heat flux is increased with surface temperature and it is known as the film boiling regime. The heat transfer coefficient in film boiling is much lower than in nucleate boiling, hence is generally considered to be inefficient. In the design of heat exchangers, film boiling is usually avoided.

Wang and Dhir[2] investigated the active nucleation sites on a heating surface. They found that the condition for gas/vapor entrapment from preexisting nuclei can be stated as

$$\phi > \varphi_{\min} \tag{1}$$

where $\varphi_{\min}$ is the minimum cavity side angle of a spherical, conical or sinusoidal cavity. The minimum superheat corresponds with the minimum diameter of curvature which equals the diameter of the cavity mouth. The corresponding expression for incipient superheat is obtained as

$$\Delta T = \frac{4\sigma T_{sat}}{\rho_v h_{fg} D_c} K_{max} \tag{2}$$

where ΔT , σ , T_{sat} , ρ_v, h_{fg} and D_c are correspondingly wall superheat, liquid surface tension, saturated temperature, vapor density, latent heat and minimum diameter of a cavity. For a spherical cavity, the K_{max}, is expressed as

$$K_{max} = 1 \text{ for } \phi \leq 90° \text{ and } K_{max} = sin\phi \text{ for } \phi > 90° \tag{3}$$

The cumulative number density of active nucleation sites for a contact angle ϕ can be expressed by surface cavity size distribution as

$$N_a = \frac{1-\cos\phi}{1-\cos\varphi} \cdot N_{as}(\varphi) \tag{4}$$

where $N_{as}(\varphi)$ is surface cavity density with a cavity mouth angle less than φ and φ is any reference cavity side angle.

In the isolated bubble regime, transient conduction into liquid adjacent to the wall is probably the most important mechanism for heat removal from the wall. After bubble inception, the superheated liquid layer is pushed outward and mixes with bulk liquid. The bubble acts like a pump in removing hot liquid from the surface and replacing it with cold liquid. This mechanism was originally proposed by Forster and Grief[3].

Mikic and Rohsenow[4] were the first to formalize the derivation of functional dependence of partial boiling heat flux on wall superheat. Assuming that the contribution of evaporation to total heat removal rate was small they obtained an expression for the partial nucleate boiling heat flux as

$$q = \frac{K_o^2}{2}\sqrt{\pi \cdot k_l \cdot \rho \cdot C_{pl} \cdot f}\; D_d^2 N_a \Delta T + \left(1 - \frac{k_o^2}{4} N_a \pi D_d^2\right) h_{nc} \Delta T \quad (5)$$

In this equation, the parameter K_o is reflective of the area of influence of a bubble, and a value of 2 is assigned to it. The bubble diameter of bubble departure and frequency, *f*, is obtained from the following correlation:

$$f D_d = 0.6 \left[\frac{\sigma \cdot g(\rho_l - \rho_g)}{\rho_l^2}\right]^{1/4} \quad (6)$$

For the natural convection heat transfer coefficient, any of the correlation available in the literature could be used.

According to Gaertner[1], most evaporation occurs at the periphery of vapor stems in the fully developed nucleate boiling regime. Energy of the phase change is supplied by the superheated liquid layer in which the stems are implanted. A time and area average model for fully developed boiling has been proposed by Dhir and Liaw[5], who assumed that vapor stems provide a stationary interface. Energy from the wall is conducted into the liquid layer and utilized in evaporation at the wall is conducted into the liquid layer and utilized in evaporation at the stationary liquid-vapor interface. The heat transfer rate into the thermal layer and the temperature distribution in the thermal layer is obtained by solving a two-dimensional steady state conduction equation. The geometry of the vapor stem adjacent to the wall is related to the contact angle and hence surface wettability can be quantitatively related to heat transfer. Employing experimentally observed void fractions and assuming nucleation site density as function of heat flux, the investigators were able to predict nucleate boiling heat flux and critical heat flux for different contact angles.

The phenomenon of film boiling is very similar in nature to film condensation. The correlations of the Nusselt number for laminar film condensation can be used for laminar film boiling with liquid properties replaced by vapor properties and adjustments made in multiplying constants.

During the 1970s and 1980s significant advances were achieved in the development of enhanced boiling surface. The enhanced surface consists of two basic types, as described by Webb[6], which are “structured” surface and “porous coated” surface. These types of enhanced surface are capable of providing a threefold to fivefold improvement in boiling heat transfer[7]. However, despite initial claims to the contrary, the use of these commercial surfaces does not appear to eliminate the superheat excursion encountered in the boiling of highly-wetting liquids. You *et al.*[8] reduced the incipient superheat by epoxying (UV-cured) several layers of fine alumina particles (0.3 to 3 micron diameter) onto an alumina heater.

The addition of certain amounts of surfactants in a aqueous solution has been known to

significantly enhance the boiling heat transfer of water. The mechanism is still not understood.

In a given heating surface and system pressure, the boiling heat flux depends on the liquid and vapor properties as discussed above. There is little difference in thermodynamic properties between bulk water and a water cluster which Lo *et al.*[9] described and called I_E crystal. The purpose of this study is to show if I_E water changes the boiling phenomenon due to its unique cluster structure. Since most of the thermodynamic properties of I_E water are not available, the mechanism of the enhancement of boiling heat transfer of I_E water is not explained.

2. EXPERIMENTAL SETUP AND PROCEDURES

2.1 Apparatus and Preliminary Work

The apparatus used in this study was intended to measure heat flux and wall superheat in all regimes of boiling (i.e., nucleate, transition and film boiling). The apparatus also allowed observation of the boiling process from front and side.

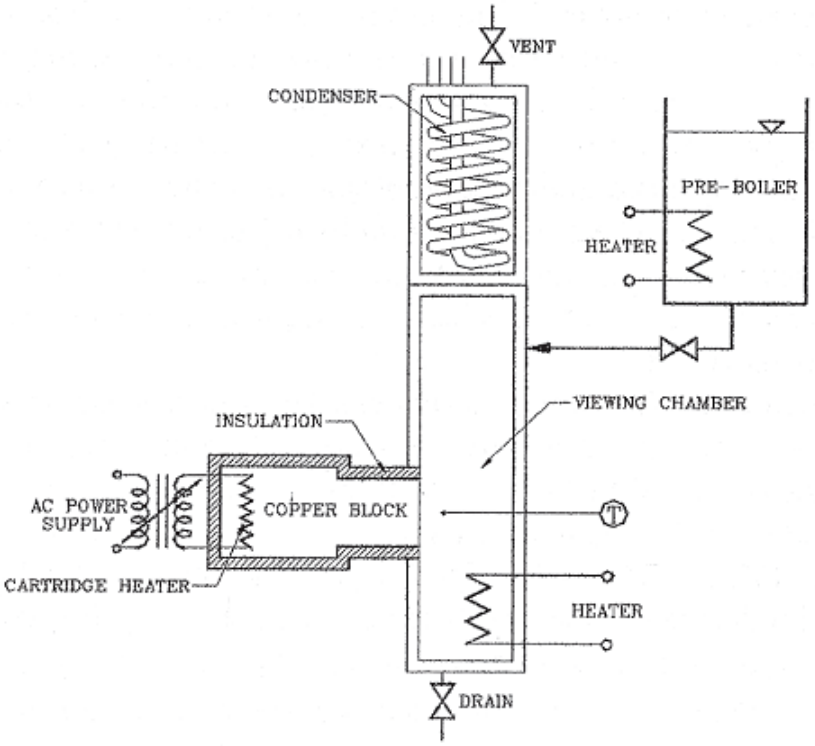

Figure 1 : Schematic diagram of primary experimental apparatus

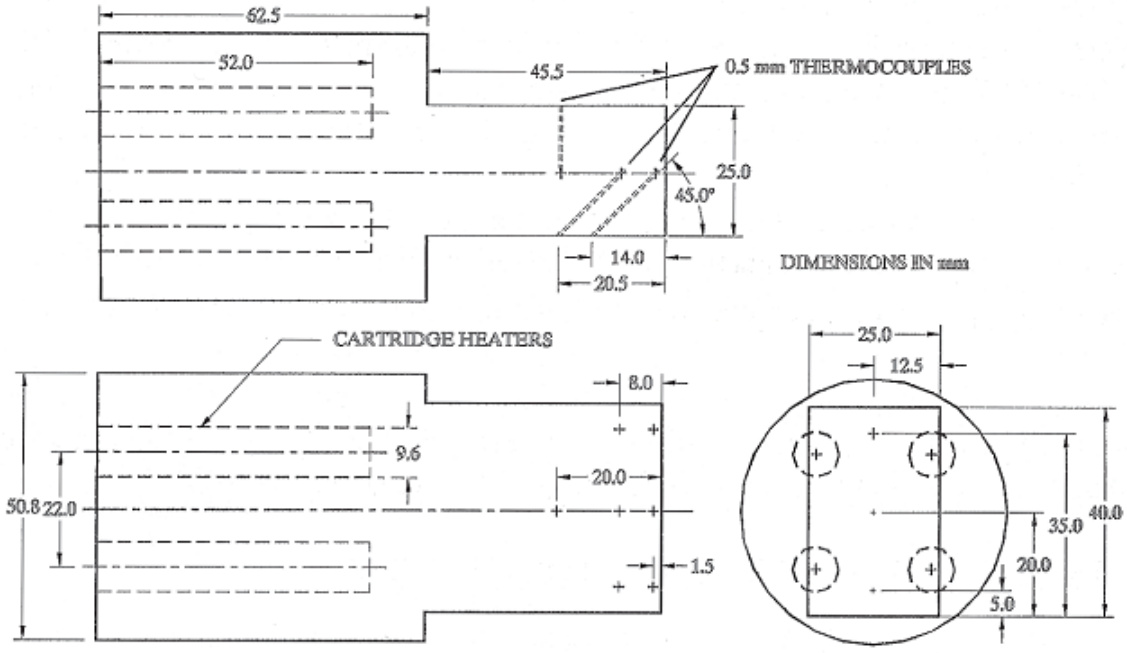

Figure 2 : Location of thermocouples in the test block

Experiments were conducted using deionized water (herein after referred to as water) and I_E Crystal aqueous solution (herein after referred to as I_E water) to study saturated pooling boiling at atmospheric pressure. The schematic diagram of the primary experimental apparatus is found in Figure 1. The test section was mounted on one side of the viewing chamber and polycarbonate sheets were placed on the remaining three sides. The rectangular heating surface was 25 mm wide and 40 mm high, and was machined from one end of a pure solid copper cylinder. The other end of the block was drilled to fit four cartridge heaters, rated at 400W each.

Figure 2 shows the dimensions of the test section and the locations of the various thermocouples. The test block projected into the viewing chamber. Since boiling on only the test surface was desired, the remaining heated areas were isolated from the test chamber. Seven K-type thermocouples were positioned along the vertical axis of the rectangular boiling surface at three locations: 5, 20, and 35 mm from the leading edge, respectively. At the edge of the first two locations, thermopiles were embedded normal to the surface at 1.5 and 8 mm from the surface. The central location, which was at 20 mm from the bottom, has extra thermopiles at 20 mm from the surface. The test surface was a mirror finish surface condition.

The chamber's windows were made of polycarbonate and were 6.4 mm thick. A Sony camcorder with a 50 mm macro lens was mounted near the chamber's window, to photograph the front view of the bubbles and vapor jet from the surface. During the boiling test, the boiling process was continuously recorded by the camcorder.

2.2 Experimental procedure

I_E water was prepared from highly purified water with a resistivity of 18 $M\Omega \cdot cm$ and the total amount of dissolved solids was less than 10 ppb by a special proprietary process.

Prior to the experiment, the test liquids were (water or I_E water) deaerated by vigorous boiling in a separate reservoir. Thereafter the test section was preheated and the chamber was filled with the test liquid from the reservoir. The power to the cartridge heaters was controlled with a transformer. Tests were considered to be in a steady state when the temperatures along the central test section did not deviate the linear distribution over 0.2K. The wall superheat was obtained by extrapolating the known temperature profile under steady state conditions. During the transient heating transition boiling, the test section was heated by gradually increasing the input power until the critical heat flux was reached. Then, the power was reduced to avoid overheating of the test block. In the test, the temperatures were recorded with a Data Acquisition System at 10Hz. The heat fluxes in steady or transient state were deduced from the recorded temperature.

In steady state tests, surface heat fluxes are readily calculable using the spatial temperature distribution recorded from thermocouples. One-dimensional heat flow was found to exist inside the test block up to 20 mm from the boiling surface. The heat flux is proportional to the negative of the temperature gradient:

$$q = -k\frac{dT}{dx} \tag{7}$$

The surface temperature was obtained by simply extrapolating the temperature profile to the surface. The q versus ΔT relation for transient runs was reduced from the temperature versus

time data by solving one dimensional conduction equation. One-dimensional heat conduction equation is written as

$$T_t = kT_{xx} \tag{8}$$

Two boundary conditions are applied at x=1.5 and 20.0 mm from the boiling surface. The initial condition and boundary conditions are expressed as

$$T(x,0) = ax + b$$
$$T(x = 1.5mm, t) = g_1(t)$$
$$T(x = 20.0mm, t) = g_2(t)$$

The one dimensional conduction equation is solved numerically. The Crank Nicolson formula with a weighting factor of $^1/_2$ is used in time discretization to assure unconditional stability. Peaceman-Rachford's ADI scheme is used in spatial splitting, as it is accurate to second order in both time and space. The surface temperature and heat flux are obtained by using Gregory-Newton forward extrapolation formula.

The uncertainty in wall superheat for nucleate and film boiling was estimated to be ±0.3K. For partial nucleate boiling and film boiling, the uncertainty in heat flux was calculated to be approximately 0.5 W/cm^2. Uncertainty in fully developed nucleate boiling heat flux was only about 1% because of high heat flux and low wall superheat. During the transition boiling, the uncertainty of temperature was not only found in x but also in z direction. Therefore, uncertainty in wall superheat was estimated to be ±1.2K and heat flux was bounded by two times the film and nucleate boiling values. During the data reduction, the time elapsed was stamped on data sheets of wall superheat and heat flux. Based on the time stamped, the still pictures corresponding to the wall superheat and heat flux were captured from camcorder.

3. RESULTS AND DISCUSSION

3.1 Wall Superheat and Heat flux

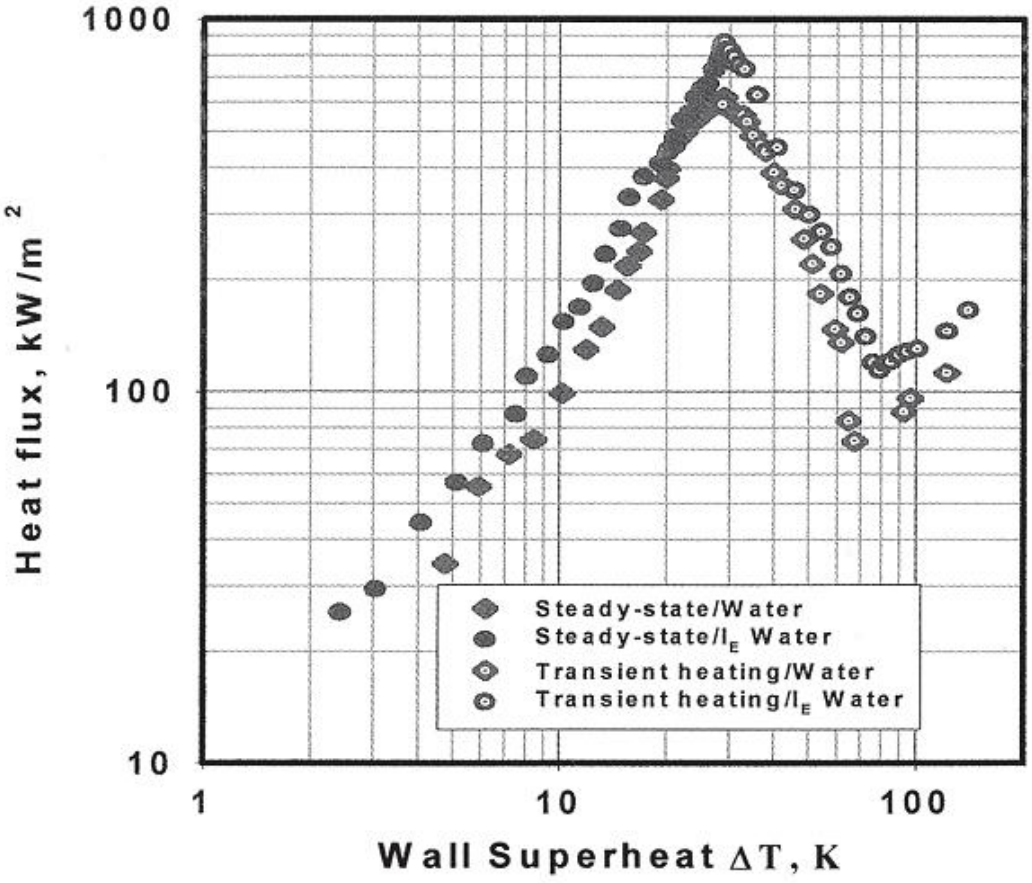

Figure 3 :Comparison of boiling curve between I_E water

During saturated pool boiling of water and I_E water, data were taken for wall superheat and heat flux. Figure 3 shows the obtained boiling curves under a mirror copper surface with a 90° contact angle. The reported data are for the mid-plane of the test surface. The nucleate boiling data were taken under steady state conditions, whereas the transition and film boiling data were obtained under transient conditions. The transition and film boiling heat fluxes were obtained from the thermocouple data by solving transient one dimensional conduction equations. In the partially nucleate boiling region where heat fluxes were under 150 kW/m2, the heat flux for a given superheat of I_E water was higher than that of water. For a given heat flux, the superheat of I_E water was up to 3.5K, lower than that of water. In fully nucleate boiling region, where heat flux was above 150 kW/m^2, it was also shown that the heat flux with a given superheat of water clusters is higher than that of water. The maximum heat fluxes for I_E water and water were 870 and 602 kW/m^2, respectively. In the transition region, where superheat was between 28 and 170 K, the heat flux curve of I_E water was always higher than that of water. In the film boiling region where superheat is over 170K, the heat flux curve of I_E water was higher than that of water

3.2 Bubble formation /Partially Nucleate Boiling

Figure 4 shows the comparison of bubble formation from the front view in the partial nucleate boiling between I_E water and water. In this region, the bubbles leaving the heating surface were single separated bubbles. When the wall superheat attained 6K, the boiling incipient occurred for both test liquids. However, there were more bubbles formed in the heating surface of I_E water than that of water. Naturally, the heat flux of I_E water was higher than that of water. When the wall superheat increased to 8.1 K, the heating surface of I_E water was almost covered by bubbles, but the bubble formation of the heating surface with water was only similar to that of I_E water at wall superheat of 6.0K. When the heating surface increased to 10.2K, the heating surface with I_E water was totally covered by bubbles and the heat flux was up to 154 kW/m^2. At the same wall superheat, the heat flux of the heating surface with water was only 99 kW/m^2. The following table compares the heat flux of water and the heat flux of I_E water at the same wall superheat. The enhanced boiling heat transfer with I_E water is between 30.9 and 55.6 %.

Table 1: Comparison of heat flux in partial nucleate boiling region

	Water	I_E water	Increasing heat flux
Superheat, ΔT (K)	Heat flux, q kW/m^2	Heat flux, q kW/m^2	%
6.0	55	72	30.9
8.1	71	110	54.9
10.2	99	154	55.6

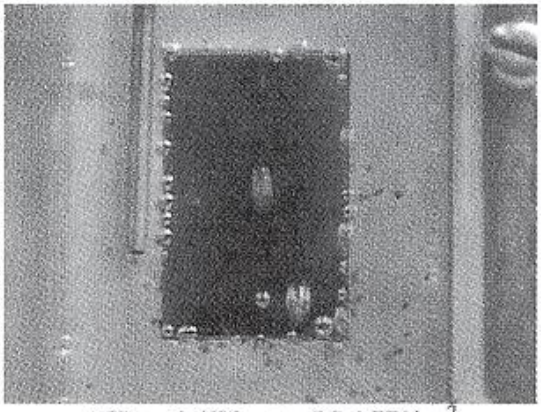

$\Delta T = 6.0K,\ q=55\ kW/m^2$

Fig. 4-1a Water

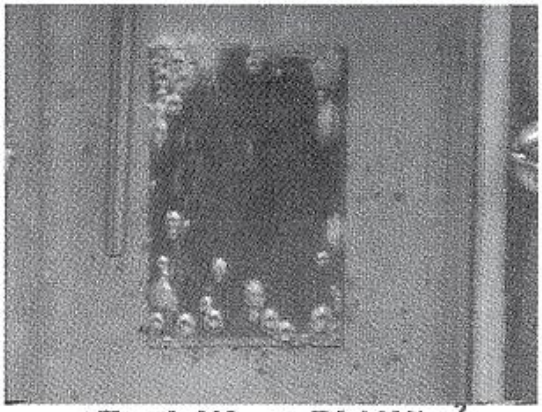

$\Delta T = 6.0K,\ q=72\ kW/m^2$

Fig. 4-1b I_E water

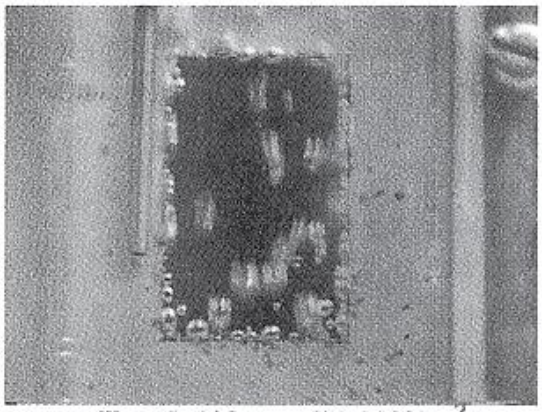

$\Delta T = 8.1K,\ q=71\ kW/m^2$

Fig. 4-2a Water

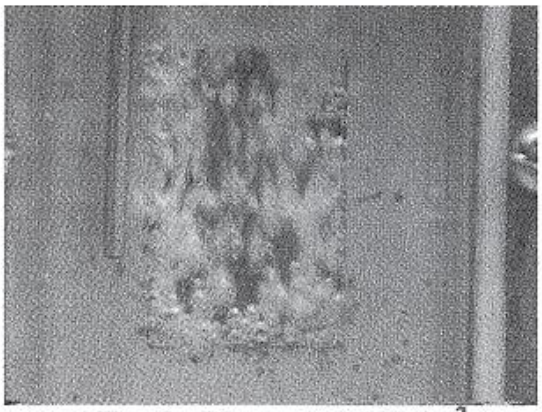

$\Delta T = 8.1K,\ q=110\ kW/m^2$

Fig. 4-2b I_E water

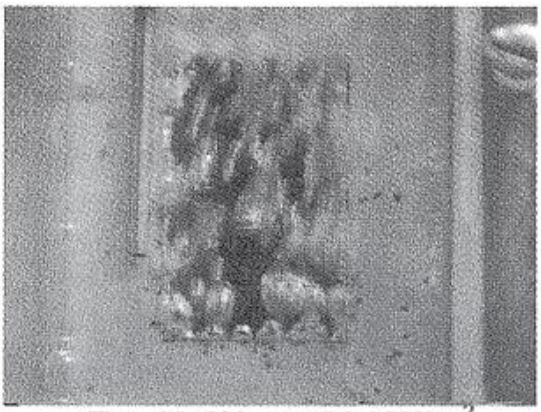

$\Delta T = 10.2K,\ q=99\ kW/m^2$

Fig. 4-3a Water

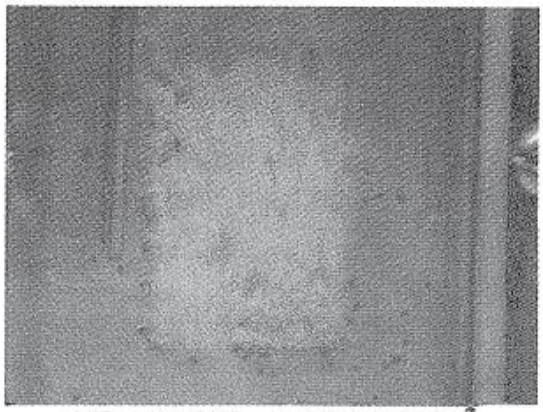

$\Delta T = 10.2K,\ q=154\ kW/m^2$

Fig. 4-3b I_E water

Figure 4 : Comparison of bubble formation in partially nucleate boiling

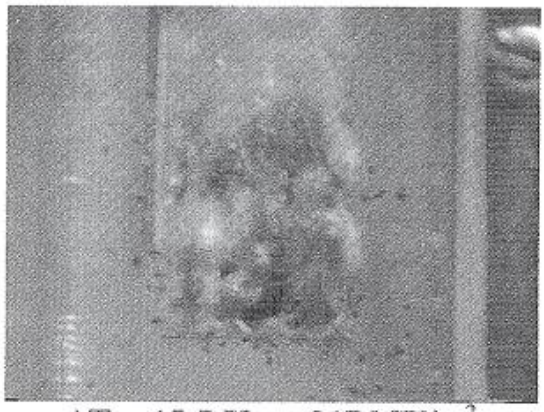

$\Delta T = 15.5$ K, $q=217$ kW/m^2

Fig. 5-1a Water

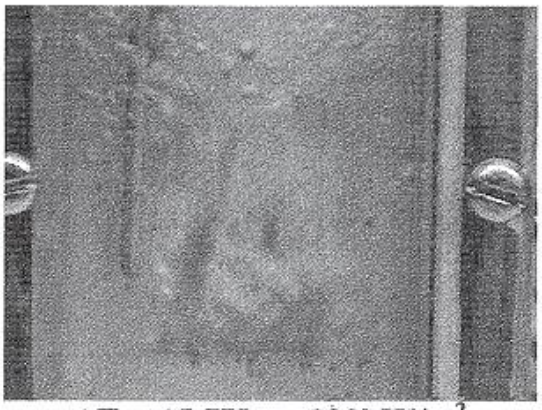

$\Delta T = 15.7$K $q=333$kW/m^2

Fig. 5-1b I_E water

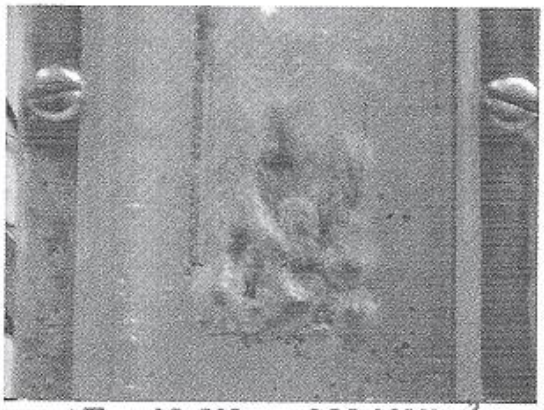

$\Delta T = 19.3$K $q=328$ kW/m^2

Fig. 5-2a Water

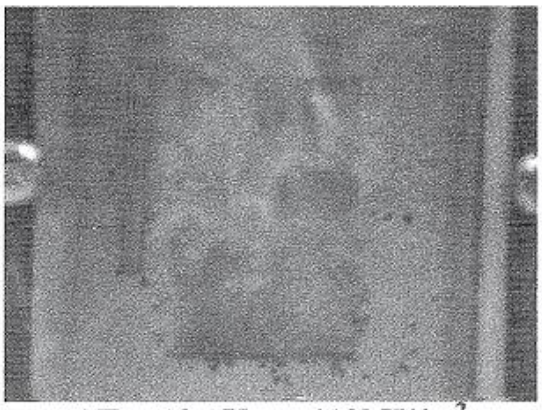

$\Delta T = 19.1$K $q=410$kW/m^2

Fig. 5-2b I_E water

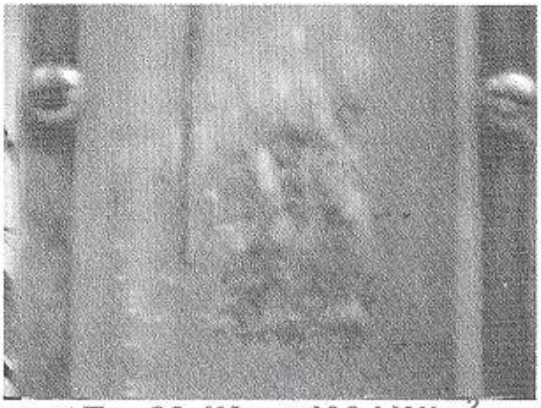

$\Delta T = 22.4$K $q=499$ kW/m^2

Fig.5-3a Water

$\Delta T = 22.0$K $q=535$kW/m^2

Fig. 5-3b I_E water

Figure 5 Comparison of vapor stem in fully nucleate boiling

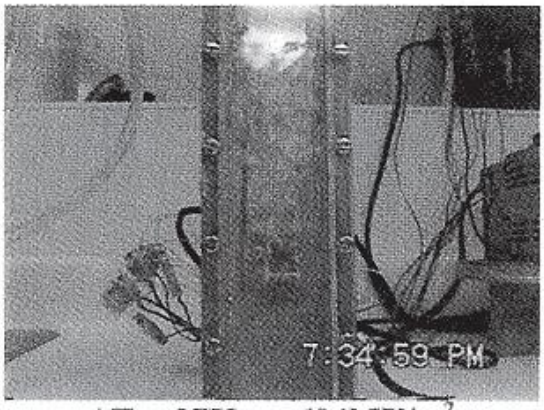

$\Delta T = 27K$, $q=604 kW/m^2$

Fig. 6a Water critical heat flux

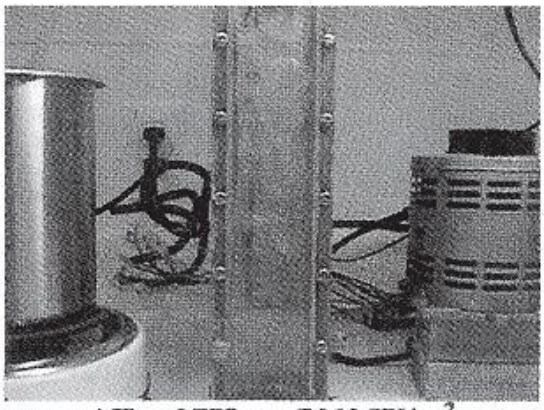

$\Delta T = 27K$ $q=733 kW/m^2$

Fig.6b I_E water fully developed nucleate boiling

3.3 Stem Formation/Fully Nucleate Boiling

Figure 5 shows the comparison of bubble formation from front view in the fully nucleate boiling between I_E water and water. In this region, the bubbles leaving the heating surface were continuous and acted as a steam jet. For all three different wall superheats, the wall heat flux of I_E water was higher than the heat flux of water. The comparison of Figures 5-lb and 5-2a indicates that the wall superheat of the heating surface with I_E water was 2.6K less than that with water as the same heat flux, of approximately 330 kW/m^2. Also, the steam jet of the heating surface with I_E water was uniformly distributed over the surface. The steam formation on the heating surface with water was more mushroom shaped (Figure 5-2a). The flow pattern difference between I_E water and water may be caused by the thermal conductivity of I_E water changing during boiling agitation. The following table compares the heat flux of water and the heat flux of I_E water at the same wall superheat. The enhanced boiling heat transfer with I_E water is between 7.2 and 53.4 %.

Table 2: Comparison of heat flux in fully nucleate boiling region

	Water	I_E water	Increasing heat flux
Superheat, ΔT (K)	Heat flux, q kW/m^2	Heat flux, q kW/m^2	%
15.5/15.7	217	333	53.4
19.3/19.1	328	410	25.0
22.4/22.0	499	535	7.2

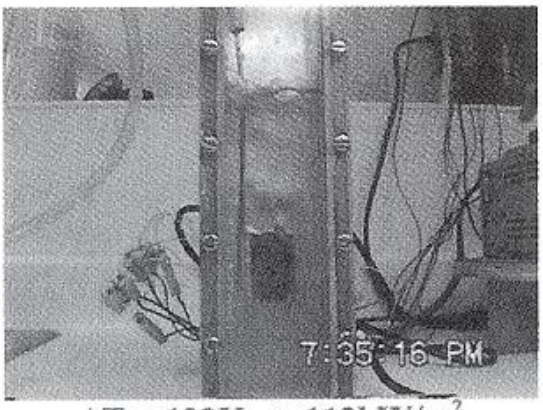

$\Delta T = 122K$ $q=112kW/m^2$

Fig. 7a Water film boiling

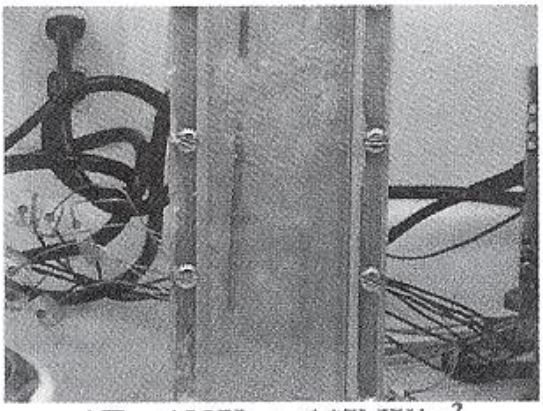

$\Delta T = 122K$ $q=145kW/m^2$

Fig. 7b I_E water film boiling

3.4 Maximum Heat Flux and Film Boiling

Figure 6a shows the front view of the heating surface with water at the critical heat flux of 604 kW/m^2 with wall superheat of 27K. At the same wall superheat (Figure 6b) shows the front view of the heating surface with I_E water at a heat flux of 733 kW/m^2. At the high heat flux, the surface is obscured by the steam mushroom formation. Above the heating surface, the flow pattern of heat flux with I_E water was different from the flow pattern of heat flux with water. The former was like bubble jets while the latter was like steam slugs.

Figures 7a and 7b show the front view of the heating surface with water and I_E water at wall superheat 122K during film boiling region. The films were formed at the heating surface with water and with I_E water. The heating surface with water was covered with a clear film; however, the heating surface with I_E water was covered with a film topped with tiny bubbles. The flow pattern above the heating surface was also different. Huge bubble slugs were continuously generated from the heating surface with water, but steam bubbles were formed above the heating surface with I_E water. The heat flux of the heating surface with I_E water was 19% higher than that with water at the same wall superheat. Since the phenomenon of film condensation on immersed plates is very similar in nature to film boiling, it is implied that enhanced film condensation can also be obtained.

4. SUMMARY AND CONCLUSIONS

1. In a nucleate boiling region, I_E water enhances the boiling heat transfer up to 56%.
2. The critical heat flux with I_E water is enhanced by 39%.
3. In a film boiling region, I_E water enhances the boiling heat transfer by 19%.
4. More bubbles are formed on a heating surface with I_E water than on a heating surface with water in nucleate boiling regime.
5. Flow pattern, above the heating surface with I_E water, is more like bubble clusters and flow pattern above the heating surface with water is more like a slug or a slug annular in film boiling regime.

5. REFERENCES

1. R.F. Gaertner, *J. Heat Transfer*, **87**, 17-29 (1965).
2. C. Wang and V.K. Dhir, *J. Heat Transfer*, **115**, 670-679 (1993).
3. D.E. Forster and R. Greif, 1959, *Heat Transfer to a Boiling Liquid-Mechanism and Correlation, ASME .1 Heat Transfer*, **81**, 43-53.
4. B.B. Mikic and W.M. Rohesenow, *ASME J. Heat Transfer*, **91**, 245-250 (1969).
5. V.K. Dhir and S.P. Liaw, *ASME J. Heat Transfer*, **111**, 739-746 (1986).
6. Webb, R.L., *Heat Transfer Engineering*, **2**, No.4-4, 46-69 (1981).
7. K. Nishikawa, *Proceedings ASME/JSME Thermal Engineering Joint Conference, JSME, Tokyo, Japan*, **3**, 11-20 (1983).
8. S.M. You, et al., *Proceedings, IEEE/ASME ITERM III, IEEE Catalog Number 92CH3096-5, New York*, 66-73 (1992).
9. S.Y. Lo, et al., *Modern Physics Letters B*, **10**, No. 19, 921-930 (1996).